星载遥感相机焦面窗口玻璃辐射热差消除设计

李永昆[1]，高长春[1]，焦建超[1]，吴立民[1]，于振涛[2]

(1. 北京空间机电研究所，北京 100094；
2. 海军潜艇学院，山东 青岛 266000)

摘　要：应某星载高精密遥感相机的功能指标要求，镜头及焦面探测器工作在不同温度，且存在较大温差，以致焦面探测器窗口玻璃的冷辐射使镜头最后一片透镜的温度梯度、面型参数等发生较大变化，不能满足光学系统成像质量的要求。为消除焦面探测器窗口玻璃的冷辐射对光学系统的影响，提出了一种于焦面探测器窗口玻璃与镜头间增加一层阻隔光窗的设计，用于将焦面窗口玻璃的冷辐射进行阻隔屏蔽，从而使光学系统的成像质量达到要求。经过建模仿真对比，证明文中的设计形式能够消除焦面组件与镜头组件间的辐射热差，提升了相机的成像质量，验证了该设计的正确性与合理性，为星载高精密相机消除部组件间的辐射热差设计起到了一定的指导作用。

关键词：高精密遥感相机；　辐射热差；　阻隔光窗；　建模仿真

中图分类号：V447+.1　　**文献标志码：**A　　**DOI：**10.3788/IRLA20230257

0　引　言

随着空间探测技术的不断发展，星载高分辨率遥感相机对光学系统的成像质量提出了越来越严苛的要求，空间环境及相机内光机结构的变化均会对光学系统的成像质量产生影响。而温度是影响光学系统性能的重要参数，温度变化会使相机光学元件及其支撑结构产生温度梯度，造成光学元件的曲率半径、中心厚度、空气间隔、折射率等发生较大变化，产生热应力和热变形，尤其是光学元件边缘区域，甚至会出现所谓的“塌边”及“翘曲”现象，导致光学元件倾斜、像面漂移以及调制传递函数 (MTF) 下降等一系列问题，引起镜头离焦，造成整个光学系统失准，因此必须要对相机进行控温及消热差设计[1−4]。

传统机电消热差及光学消热差原理均通过改变镜组的轴向偏移量，从而实现各光学元件在温度变化时的动态离焦量相互抵消补偿，使光学系统各镜面在温度变化时保持相对稳定，实现优良的像质。

上述消热差设计均基于热传导原理，适用于消除由相机整体温度变化引入的温度梯度而造成光学元件镜面偏移的影响，文献 [5−10] 均采用这一原理。而上述文献中未考虑镜头各组件之间的热辐射影响，目前基于其他部组件热辐射引入的温度梯度对光学系统像质产生的影响研究较少。

文中基于某星载遥感相机因镜头与焦面探测器工作温差较大，致使镜头最后一片透镜受焦面探测器窗口玻璃冷辐射而产生光学成像质量所不能接受的面型参数变化开展研究，提出了一种消除焦面窗口玻璃辐射热差的设计，并通过仿真分析验证了该设计的正确性与合理性。

1　物理模型

某星载遥感可见光相机的基本组成如图 1 所示，主要包括遮光罩组件、镜头组件、焦面组件及散热面组件四个部分。光学信号源通过遮光罩组件后进入镜头组件，经过 8 个透镜组的调制与过滤成像于焦面探测器上，完成成像信息的接收、调制和转换。

依据成像功能指标要求，焦面探测器需要在低温低噪声状态下完成对目标的精密监视探测，其最适工作温度为−20 ℃，实际工作时需要将其工作温度控制在 (−20±2) ℃。然而镜头各透镜组件需要在 20 ℃ 的最适工作温度下维持其面型参数，保证相机成像质

收稿日期：2023−04−26；　**修订日期：**2023−07−10

作者简介：李永昆，男，工程师，硕士，主要从事空间遥感相机光机结构设计与仿真方面的研究。

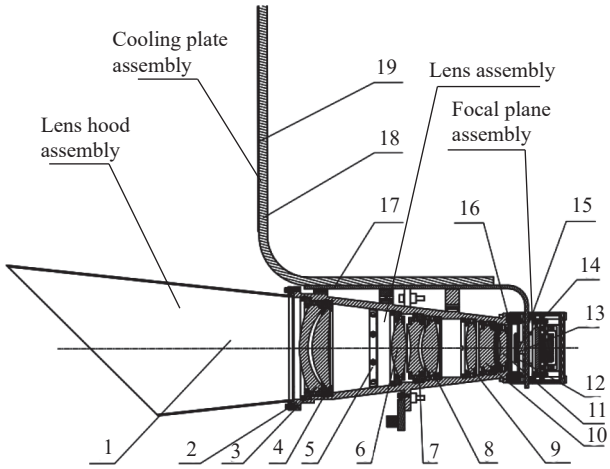

1—Hood; 2—Lens cone; 3—Mirror 1; 4—Mirror 2; 5—Diaphragm; 6—Mirror 3; 7—Mirror 4;
8—Mirror 5; 9—Mirror 6; 10—Mirror 7; 11—Mirror 8; 12—Focal surface window; 13—Focal detector;
14—Heat-conducting plate; 15—Copper plate; 16—Focal surface gasket;
17—Focal surface small heat pipe; 18—Focal surface big heat pipe; 19—Cooling plate

图 1 相机基本组成

Fig.1 Composition of camera

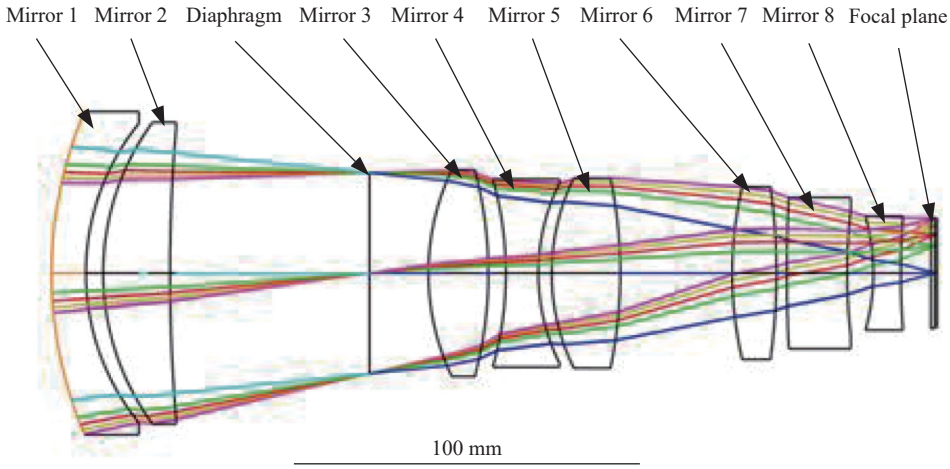

图 2 光学系统成像模型

Fig.2 Optical system imaging model

量，镜头组件实际工作时控制其温度为 (20±2) ℃，这样在焦面组件与镜头组件之间便产生了 40 ℃ 的工作温差，二者结合处具有较大的温度突变[11−12]。

相机光学系统成像模型如图 2 所示，成像谱段为 420~700 nm。由图可知，相机光学后焦距较短，以致透镜 8 组件 (图 1 中 11) 与焦面探测器 (图 1 中 13) 直接相对且距离较近，仅为 7.07 mm。探测器表面安装着焦面窗口玻璃 (图 1 中 12)，当探测器在 (−20±2) ℃ 下稳定工作时，窗口玻璃对外的冷辐射使透镜 8 产生了超出相机指标要求的温度梯度，引起透镜光学参数发生变化，造成镜面偏移，最终导致光学系统像质下降。

以单透镜为例，当温度变化 Δt 时，变化后的透镜参数可表示为如下形式。

透镜厚度：

$$d' = d + \mathrm{d}d = d(1 + a_0 \cdot \Delta t) \tag{1}$$

前表面曲率半径：

$$r_1' = r_1 + \mathrm{d}r_1 = r_1 + 0.5d \cdot a_0 \cdot \Delta t \tag{2}$$

后表面曲率半径：

$$r_2' = r_2 + \mathrm{d}r_2 = r_2 + 0.5d \cdot a_0 \cdot \Delta t \tag{3}$$

空气折射率:

$$n_{air}' = n_{air} + \mathrm{d}n_{air} = n_{air} + \beta_{air} \cdot \Delta t \tag{4}$$

式中: a_0为透镜热膨胀系数; β_{air}为空气折射率温度系数。

定义温度焦距位移系数 T 为单位光焦度透镜在单位温升后的光焦度改变量, 则有:

$$T = \frac{1}{\varphi}\frac{\mathrm{d}\varphi}{\mathrm{d}t} = \frac{1}{n - n_{air}}\left(\frac{\mathrm{d}n}{\mathrm{d}t} - n \cdot \frac{\mathrm{d}n_{air}}{\mathrm{d}t}\right) - a_0 \tag{5}$$

因此, 较大的温差梯度引会起透镜面型参数如曲率半径、中心厚度、折射率等发生较大变化, 造成面型偏移[13−16]。热差分为位置热差和倍率热差, 前者定义为温度变化前后轴上物点成像位置的差异; 后者定义为温度变化前后因成像倍率变化造成的像大小的差异。两类热差的表达式可通过与初级色差类似的推导方法得到, 分别表示为:

$$\Delta l_{th}' = -\frac{1}{n_k' u_k' 2}\sum_{1}^{k+1} H_{\mathrm{I}} \tag{6}$$

$$\Delta y_{th}' = -\frac{1}{n_k' u_k'}\sum_{1}^{k+1} H_{\mathrm{II}} \tag{7}$$

式中: $\Delta l_{th}'$为位置热差; H_{I}为初级位置热差系数; n_k'为系统像方折射率; u_k'为系统像方孔径角。

透镜中心厚度引起的矢高增量为:

$$\Delta h = D^2 \cdot \alpha \cdot \Delta T / 8d \tag{8}$$

式中: D 为透镜口径的等效平板口径; ΔT为表面温差; α为热胀系数; d 为等效平板玻璃厚度。当焦距为 f (f=148 mm) 时, 对应于矢高增量Δh的焦距改变量 Δf 如下:

$$\Delta f = 2f^2 \cdot \alpha \cdot \Delta T / d \tag{9}$$

透镜 8 的材料为 H-FK61, 代入相关数据, 计算得到透镜 8 的矢高变化量为 0.07 mm, 镜面焦距变化量为 6.88 mm, 矢高及焦距变化百分比分别为 1.4% 和 4.6%[17−19]。

镜头设计的 MTF 及由于窗口玻璃冷辐射影响后的 MTF 如图 3 所示。对比可知, 镜头光学系统设计的 MTF 约为 0.78, 而由于冷辐射引起透镜 8 的面型参数发生变化, 致其 MTF 降为 0.57, 已不能满足镜头 MTF 为 0.72 的指标要求, 因此必须将焦面组件与镜头组件间的辐射热差进行消除。

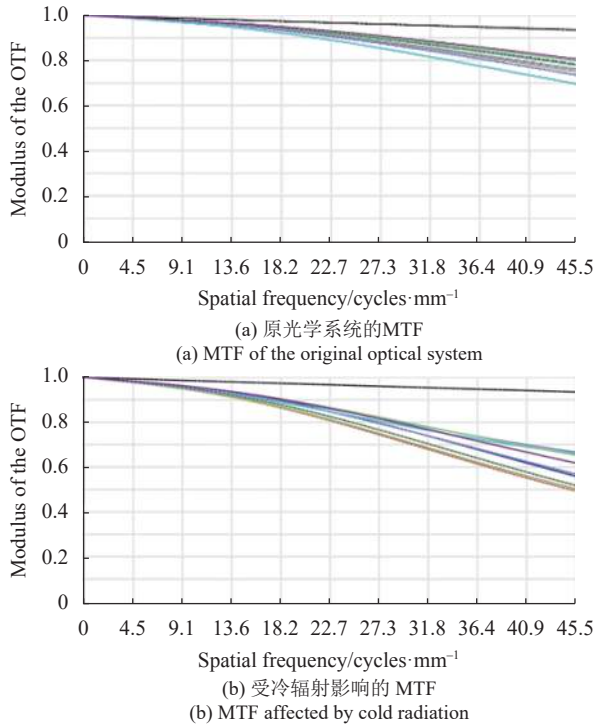

(a) 原光学系统的MTF
(a) MTF of the original optical system

(b) 受冷辐射影响的 MTF
(b) MTF affected by cold radiation

图 3 镜头 MTF 对比图

Fig.3 Contrastive MTF of lens

2 消除热差设计

为了消除焦面窗口玻璃对透镜 8 的冷辐射影响, 于焦面探测器窗口玻璃与透镜 8 组件之间设计增加阻隔光窗, 如图 4 中 10 所示, 其固定连接在焦面盒壳

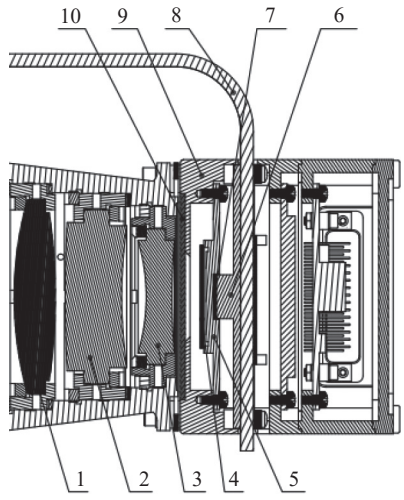

1—Mirror 6; 2—Mirror 7; 3—Mirror 8; 4—Focal surface window
5—Focal detector; 6—Copper plate; 7—Heat-conducting plate;
8—Focal surface small heat pipe; 9—Focal box housing;
10—Light blocking window

图 4 阻隔光窗设计

Fig.4 Light blocking window design

体 (图 4 中 9) 上，通过对焦面盒进行主动控温，使连接在其上的阻隔光窗温度稳定在 14 ℃，这样便在焦面探测器与透镜 8 组件之间形成了辐射屏障，从而阻隔焦面窗口玻璃的冷辐射，使透镜 8 的面型参数得到修复。

对阻隔光窗在光学系统设计软件中进行严格的仿真计算，将由阻隔光窗的引入对光学系统透过率、光程差、附加像移及其他对成像质量的影响降为零。经多次仿真迭代计算，确定其最终设计形式及具体参数，材料选用热膨胀系数较小的熔石英 7980。

通过对焦面盒壳体进行主动控温使其温度稳定在 14 ℃，这样经热传导使固连在其上的阻隔光窗温度同样稳定在 14 ℃。如此通过 14 ℃ 的阻隔光窗便隔绝了工作在−20 ℃ 的焦面窗口玻璃的冷辐射量，从而使透镜 8 及镜头整体温差得到修复，满足光学系统的成像质量要求。

3 仿真分析

3.1 仿真模型

将整机三维模型导入到 UG NX 软件中进行有限元建模，分为增加阻隔光窗及无阻隔光窗两种有限元状态。为使有限元网格单元形状合理且便于分析，在不影响整机传热路径及光机结构热学特性的前提下，对模型进行了一系列的修改及简化操作，如：忽略结构的倒角、圆角等，得到整机有限元仿真模型如图 5 所示。

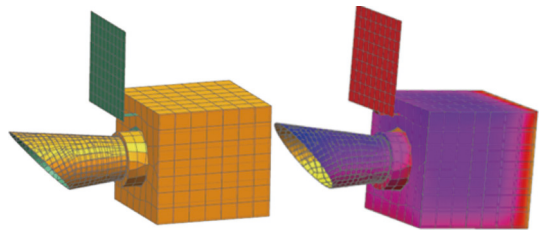

图 5 整机热仿真有限元模型

Fig.5 Finite element model of thermal simulation of whole camera

3.2 边界条件及仿真参数设置

在软件中对整机光学元件及结构件材料属性参数进行设置，所需参数主要为密度、热膨胀系数、导热率等，各材料参数如表 1 所示，其中光学元件材料参数来源于《成都光明光学玻璃数据表》。

表 1 各零件材料参数

Tab.1 Material parameters of each component

Material	Application part	Density/kg·m^{-3}	Conductivity/W·m^{-1}·K^{-1}	Expansion (10^{-6})/K
Aluminium	Focal box/Cone	2 700	117.2	10.73
7 980	Blocking window	2 200	1.38	0.51
TC4	Lens bracket	4 440	15.2	10.2
H-LAF50B	Mirror 4	4 240	-	5.8
H-ZLAF52A	Mirror 5, 7	4 480	-	6.1
H-FK61	Mirror 2, 3, 8	3 700	-	13.1
H-LAF3B	Mirror 1, 6	4 500	-	8
D263T	Focal window	2 510	-	7.2

3.3 仿真结果

镜筒及焦面盒外壳设有加热片及主动控温回路，分别将其输入边界温度设为 (20±2) ℃ 及 (14±2) ℃，焦面探测器通过两级热管及散热板向深冷空间散热，将其温度设置为 (−20±2) ℃。对整机进行热仿真分析，加阻隔光窗与不加阻隔光窗对透镜组件的对比影响结果如图 6 所示。

为使对比效果明显，将透镜 8 组件在有无阻隔光窗两种状态下的镜体中心及边缘温度对比结果整理成图 7 所示的分布曲线。

由图 7 可知，加入阻隔光窗后，使得透镜 8 的镜体温度为 18.32~19.15 ℃，镜体温差梯度从无阻隔光窗的 2.7 ℃ 减小为 1 ℃ 以内，温差提高了 1.7 ℃。1 ℃ 以内的温差梯度使透镜 8 的面型参数得到修复，

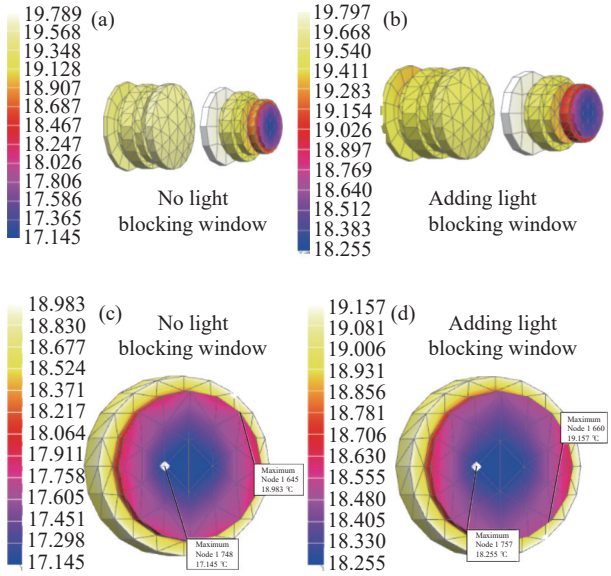

图 6 透镜 8 组件温度仿真对比云图

Fig.6 Comparative temperature simulation diagram of mirror 8

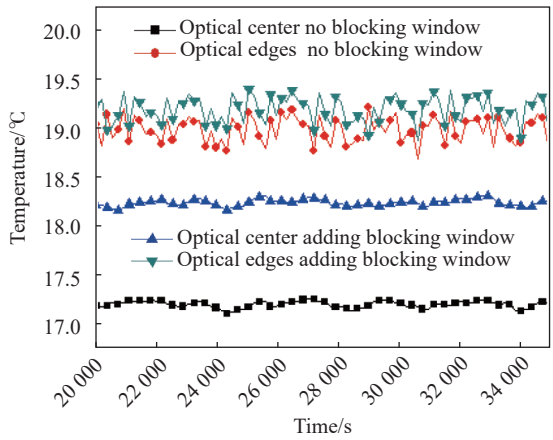

图 7 透镜 8 温度改善曲线

Fig.7 Improved temperature curve of mirror 8

修复后的面型仿真结果如图 8(a) 所示，图 8(b) 所示为加入阻隔光窗后整个镜头改善的 MTF。

由图 8 可知，1 ℃ 以内的温度梯度使透镜 8 的面

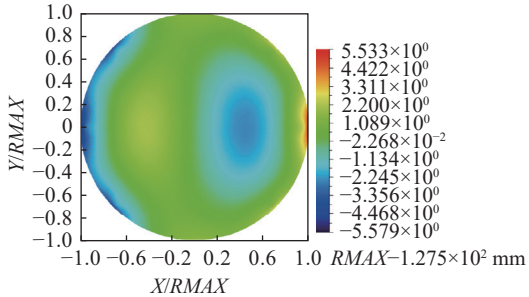

(a) 透镜 8 修复的面型

(a) Repaired surface of mirror 8

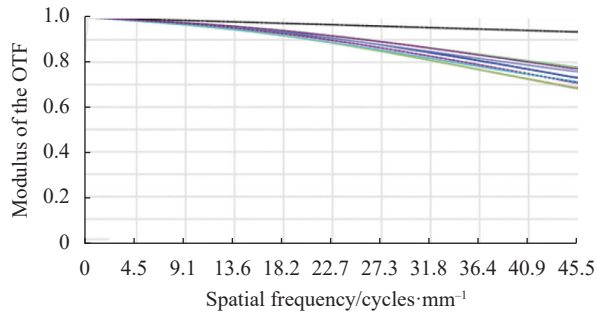

(b) 改善后的 MTF

(b) Improved MTF

图 8 透镜的热形变面型仿真结果及镜头改善后的 MTF

Fig.8 Simulation results of themal deformation of mirror and improved MTF of lens

型参数 (曲率半径、中心厚度、折射率等) 均在成像质量允许的范围内，已满足相机成像性能对透镜组的要求，并由此使得整个镜头光学系统的 MTF 由无阻隔光窗的 0.57 修复到了 0.75，提升了相机的成像质量。

4 结 论

为消除焦面探测器窗口玻璃的冷辐射对靠近其的透镜组件产生面型参数变差的影响，文中通过一种增加阻隔光窗的设计形式，将其对透镜组件的冷辐射影响进行阻隔屏蔽，从而消除由于镜头主体与焦面探测器工作温差较大所引起的辐射热差。

通过仿真数据表明，文中的设计正确可靠，与特定的消除辐射热差的机构或复杂结构相比形式简便，成本较低，避免了由于其他组件引入对光学系统成像质量引起新的问题。通过消除镜头组件与焦面组件的辐射热差，使镜头最后一面透镜的面型参数与整机光学系统的 MTF 得到较大提升，验证了该设计的正确性与合理性，可为星载高精密遥感相机消除辐射热差设计提供一定的指导作用。

参考文献：

[1] Deng Jian, Tong Weihong, An Xiaoqiang, et al. Athermalization of infrared zoom system [J]. ***Journal of Applied Optics***, 2011, 32 (1): 133-137. (in Chinese)

[2] Zhang Xuyan, Jiang Ruikai, Jia Hongguang. Athermalization of long-wave infrared optical system with large relativeaperture [J]. ***Journal of Applied Optics***, 2011, 32(6): 1227-1231. (in Chinese)

[3] Xia Zhongqiu, Huang Qiaolin, He Hongyan, et al. Analysis of geolocation accuracy of high resolution opticalremote sensing

satellite geometric chain [J]. ***Spacecraft Recovery & Remote Sensing***, 2016, 37(3): 111-118. (in Chinese)

[4] Kong Lin, Yang Lin. Study and test of thermal-defocusing property in space camera [J]. ***Optics and Precision Engineering***, 2017, 25(7): 1825-1831. (in Chinese)

[5] Wang Xuexin, Jiao Mingyin. Combination of optical passive and mechanical—electrical athermalisation [J]. ***Journal of Apllied Optics***, 2010, 31(3): 354-359. (in Chinese)

[6] Gao Ming, Liu Gang, Lu Hong. Optical passive athermalization design of long-wavelength infrared inverted telephoto objective [J]. ***Journal of Xi'an Technological University***, 2015, 35(2): 94-100. (in Chinese)

[7] Jiang Yang, Sun Qiang, Liu Ying, et al. Athermal design for ir optical seeker system with wide FOV [J]. ***Acta Photonica Sinica***, 2014, 42(4): 462-466. (in Chinese)

[8] Chen Xiao, Yang Jianfeng, Ma Xiaolong, et al. Athermalization design of wide temperature range for hybrid refractive/ diffractive infrared objective [J]. ***Infrared and Laser Engineering***, 2011, 40(1): 79-82. (in Chinese)

[9] Zhang Xin, Jia Hongguang, Zhang Yue. Optical design of athermalized infrared telephoto objective [J]. ***Infrared and Laser Engineering***, 2012, 41(1): 178-183. (in Chinese)

[10] Zhang Chunyan, Shen Weimin. Design of an athermalized MWIR and LWIR dual-band optical system [J]. ***Infrared and Laser Engineering***, 2012, 41(5): 1323-1328. (in Chinese)

[11] Liu Jun, Chen Yang. Visible/Infrared dual-band large field shared-aperture and parfocal optical system [J]. ***Journal of Xi'an Technological University***, 2014, 33(2): 87-93. (in Chinese)

[12] Yu Feng, Wang Bing, Zhao Zhenming. Influence of solar radiation parameters onoptical lens thermal design and its simulation countermeasure [J]. ***Spacecraft Recovery & Remote Sensing***, 2013, 34(2): 36-41. (in Chinese)

[13] Song Yiwei, Yu Siyuan, Tan Liying, et al. Study for the influence of space temperature field on planar mirror shape [J]. ***Journal of Astronautics***, 2010, 31(3): 68-74. (in Chinese)

[14] Wang Fuguo. Study on the influence of temperature and support style to the 1.2 m SiC primary mirror surface figure [J]. ***Acta Photonica Sinica***, 2011, 40(6): 933-936. (in Chinese)

[15] Yang Xun, Xu Shuyan, Ma Hongcai, et al. Influence of radical temperature gradient on surface figure of light weight reflective mirror [J]. ***Optics and Precision Engineering***, 2019, 27(7): 1552-1560. (in Chinese)

[16] Ji Wenchen, Zhang Yu, Huang Pan, et al. Effect of axial tenlperature gradient on optical perfbrmance of infrared lens [J]. ***Laser & Infrared***, 2015, 45(9): 1100-1104. (in Chinese)

[17] Zhou Xiaohua, Xing Hui, Yang Jukui. Epoxy selection for reflect mirror assembly in space remote sensor [J]. ***Spacecraft Recovery & Remote Sensing***, 2019, 40(3): 65-72. (in Chinese)

[18] Dong Deyi, Li Zhilai, Xue Donglin, et al. Integraled opto-mechallical analysis and experiments for influence of gravity on wavefront aberration of space camera [J]. ***Optics and Precision Engineering***, 2016, 24(8): 1917-1926. (in Chinese)

[19] He Yan, Wang Jihong, Peng Qi. Themal propeny of large aperture light primary mirror [J]. ***Opto-Electronic Engineering***, 2014, 41(6): 63-69. (in Chinese)

Design for eliminating radiant heat difference of focal surface window in spaceborne remote sensing camera

Li Yongkun[1], Gao Changchun[1], Jiao Jianchao[1], Wu Limin[1], Yu Zhentao[2]

(1. Beijing Institute of Mechanics & Electricity, Beijing 100094, China;
2. Navy Submarine Acadmy, Qingdao 266000, China)

Abstract:

In accordance with the requirements of a satellite-borne remote sensing camera, the lens and focal detector work at different temperatures, which results in a large temperature difference between them. The cold radiation of the focal detector window makes the surface parameters and temperature gradient of the lens change greatly, which cannot meet the imaging requirements. In order to eliminate the influence of radiant heat difference, this paper proposes a design of adding a light blocking window between the detector window glass and the lens, which is used to elininate the cold radiation of the focal window glass so that the imaging quality of the lens system can

meet the requirements. Through comparative simulation, it is proved that the design form of this paper can eliminate the influence of the radiant heat of the focal plane, which verifies the rationality and correctness of this design and provides a certain design guidance for the design of high-precision lens to eliminate the radiant heat difference.

Objective Temperature is an important parameter that affects the performance of the lens system of high-precision satellite-borne remote sensing camera. Temperature change produces temperature gradient, which results in thermal stress and thermal deformation. And the mirror element curvature radius, center thickness, air interval, refractive index change greatly, especially on the edge area of optical element. Even edge collapse and warping phenomenon appeared, resulting in mirror element tilt, imaging plane drift and other problems, which affects the imaging quality of camera. So athermalization design and temperature control must be adopted for remote sensing camera. Many athermalization designs are based on the temperature gradient introduced by heat conduction to affect the mirror displacement of optical elements, but the effect of temperature gradient introduced by radiant heat difference is less studied. Therefore, based on the surface parameter change of a satellite-borne remote sensing camera lens assembly caused by the cold radiation of the focal plane detector window glass, which is not satisfied for optical image quality, a design for eliminating the radiant heat difference of the focal plane window glass is proposed, which provides some guidance for the design of the radiant heat difference between the eliminating components of the satellite-borne high-precision camera.

Methods In order to eliminate the radiant heat difference between the focal plane and the optical lens, a blocking light window is designed between the focal plane detector window glass and the mirror 8(Fig.4). The blocking light window is fixed on the focal surface box shell through adhesive. Through active temperature control, the focal surface box temperature is stabilized at 14 ℃, and the temperature of the blocking light window fixed on the focal surface box shell is also stabilized at 14 ℃, so that a radiation barrier is formed between the focal plane detector and the mirror 8 components. Through the 14 ℃ blocking light window, the cold radiation of the focal plane window glass is blocked, so that the surface parameters of lens 8 and the overall temperature difference of the lens can be repaired, and the imaging quality requirements of the lens system can be met.

Results and Discussions With the addition of the light blocking window, the body temperature of mirror 8 is 18.32-19.15 ℃, the gradient temperature difference of mirror 8 is reduced from 2.7 ℃ without the blocking light window to less than 1 ℃, the temperature difference is increased by 1.7 ℃ (Fig.6). The surface profile parameters of mirror 8 can be repaired by the temperature difference gradient within 1 ℃, which can meet the requirements for camera imaging quality. As a result, the modulation transfer function (MTF) of the entire lens system is repaired from 0.57 to 0.75 (Fig.8), improving the image quality of the camera.

Conclusions In order to eliminate the influence of the cold radiation of the window glass of the focal plane detector on the surface parameter of the mirror near it, this paper adopts a design form of adding a blocking light window to block the cold radiation effect so as to eliminate the radiant heat difference between the mirror and the focal plane detector. The surface parameters of the mirror near the focal plane detector and the MTF of the whole lens system are greatly improved, which verifies the correctness and rationality of the design, and can provide a certain guidance for the design of eliminating the radiant heat difference of the satellite-borne high-precision remote sensing camera.

Key words: high-precision remote sensing camera; radiant heat difference; light blocking window; modeling simulation